Running head: Seasonal Sea-Surface CO_2

Seasonal sea-surface carbon dioxide in the Azores area

A.F. Ríos[1], F.F. Pérez[1], M. Álvarez[1], L. Mintrop[2], M. González-Dávila[3], J.M. Santana Casiano[3], N. Lefèvre[4,5], A.J. Watson[4]

[1] Instituto de Investigaciones Marinas. CSIC. Eduardo Cabello, 6. 36208-Vigo, Spain. Email: aida@iim.csic.es.

[2] Institute for Baltic Sea Research, P.O. Box 301161, D-18112 Rostock. Germany

[3] Facultad de Ciencias del Mar. Universidad de Las Palmas de Gran Canaria, Campus de Tafira. 35017 Las Palmas. Spain.

[4] School of Environmental Sciences, University of East Anglia, Norwich NR4 7TJ, United Kingdom

[4] LODYC, UMR 7617 CNRS/IRD/UPMC/MNHN, Université Pierre et Marie Curie, Tour 45-55 5ème étage, BP 100, 4 Place Jussieu, 75252 Paris cedex 05, France.

Corresponding author: Aida F. Ríos

email: aida@iim.csic.es.

Fax: +34-986292762

Phone: +34-986231930 Ext. 371

Submitted to Marine Chemistry, Revised (31 October 2004)

Keywords: CO_2 fluxes, seasonal variability, advection, mixing, air-sea exchange, biological activity, Azores.

Abstract.

The seasonal evolution of total inorganic carbon and CO_2 air-sea fluxes in the Eastern North Atlantic Subtropical Gyre (Azores area) was investigated by means of studying a data set from 10 cruises covering a seasonal cycle. Monthly CO_2 fugacity was modelled as a function of surface temperature and month for 1998. So, the seasonal cycle of CO_2 and its air-sea fluxes were obtained using monthly average surface data in the area. Over the year, the Azores area ($2.25 \cdot 10^{12}$ m^2) acts as a weak net sink of CO_2 (0.38 mmol m^{-2} d^{-1}). From December to May, the zone is a rather strong sink for CO_2 (10.3 mmol m^{-2} d^{-1}), while between June to November it behaves as a CO_2 source (9.9 mmol m^{-2} d^{-1}), August presents the highest outgassing (3.88 mmol m^{-2} d^{-1}). Moreover, a box budget was established to evaluate the relative contribution of the physical and biological processes affecting the seasonal CO_2 variability in the mixed layer of the Azores area. The most important contributor to the average mass balance of CO_2 was the mixing with the lower layer (7.8 mmol m^{-2} d^{-1}) and biological activity (–8.9 mmol m^{-2} d^{-1}). Conversely, air-sea exchange (0.17 mmol m^{-2} d^{-1}) and advection (1.7 mmol m^{-2} d^{-1}) contribute with a very small input. There is a strong coupling between biological activity, advection and mixing in the mixed layer depth. The biological activity is supported by mixing and advection that provide CO_2 and nutrients to the mixed layer, so we combine the three processes in only one term (ΔC_{AMB}) that represents the net biology production in the water

column, and re-evaluated the CO_2 mass balance to discriminate the importance of the physical and biological contributions. The effect of temperature, wind and net biological process contribute in 42%, 12% and 46%, respectively, to the explained variance of total CO_2 mass balance in the upper layer.

1. Introduction

The Subtropical gyres are convergence zones, potentially regions of CO_2 accumulation by the ocean. According to Takahashi *et al.* (2002), the uptake of CO_2 in the gyres (14ºN-50ºN and 14ºS-50ºS) represents 56% of the total ocean uptake. In the Eastern North Atlantic Subtropical Gyre, the major circulation feature is the Azores current that joins the Mid Atlantic Ridge at about 35ºN, 40ºW (Klein and Siedler, 1989). Afterwards, it flows zonally eastwards between 32 and 35ºN with three branches turning to the south between 10 and 20ºW (Sy, 1988; Stramma, 1984). The mesoscale circulation in the Azores region is dominated by the meandering of the Azores front and associated eddies (Käse and Siedler; 1982, Käse *et al.*, 1985; Gould, 1985; Pingree, 1997; Pérez *et al.*, 2003). These eddies produce an intricate vertical structure with alternate cyclonic and anticyclonic eddies at both sides of the Azores front (Pingree and Sinha, 1998).

The Azores zone shows an excess of evaporation and heat loss generated by the strong and persistent trade winds (Schmitt et al., 1989; Marshall *et al.*, 1993), contributing to an increase of salinity along the southern side of the Azores current. The presence of this saline water in the upper layer favours the water mass formation of the Madeira Mode Water (Siedler *et al.*, 1987).

The former physical features, the convergence produced by the Azores current and the formation of the Madeira Mode water, favour the uptake of

anthropogenic CO_2 in the Eastern North Atlantic Subtropical Gyre. Therefore, the Azores zone has high interest as a potential sink for atmospheric CO_2. The goal of this work is to evaluate the seasonal variability of the sea surface CO_2 and to assess the relative contribution of the physical and biological processes affecting its mass balance in the Azores area.

Several studies were carried out in the subtropical gyres to evaluate the seasonal variability of the sea surface CO_2. Follows *et al.* (1996) investigated the subduction of carbon driven by the solubility pump in the North Atlantic Subtropical Gyre using abiotic models. They concluded that the rate of subduction of carbon is strongly influenced by the gradients in mixed-layer thickness over the gyre and, to a lesser extent, modified by the winter properties for subduction. This abiotic study has neglected the role of the biological uptake of CO_2 in the euphotic zone, which also modifies the carbon distribution and drives air-sea fluxes of CO_2. Recently, Lefèvre and Taylor (2002), using a one-dimensional model in the North and South Atlantic gyres reproduced the seasonal cycle of temperature and partial pressure of CO_2 (pCO_2) to examine temporal and spatial variability. They conclude that in both gyres, the pCO_2 is mainly governed by temperature changes. Takahashi *et al.* (2002) presented a method for distinguishing the seasonal biological and temperature effects on sea surface pCO_2 discussing the relative importance of both factors in the global oceans. These studies revealed interesting aspects of the seasonal cycle of the CO_2 in the Atlantic Subtropical Gyres. However, the contribution of the biological processes on the pCO_2 has been neglected (Follows *et al.*, 1996), considered to be significant but not quantified (Lefèvre and Taylor, 2002), or discussed its relative importance on a global scale (Takahashi *et al.*, 2002). Only Bates *et al.* (1996) have considered biological uptake of CO_2 together with advection, vertical entrainment and diffusion,

and gas exchange to investigate the CO_2 seasonal variability in the Western North Atlantic Subtropical Gyre. However, the Eastern North Atlantic Subtropical Gyre is poorly known in those aspects. So, the seasonal cycle of CO_2 is investigated here, evaluating the role and relative contribution of biological activity, advection, mixing and air–sea CO_2 exchange in the Azores region.

The present work is laid out as follows: we briefly present the surface distribution of CO_2 fugacity in relation with the physical characteristics of the Azores area (Section 3.1); the following section will be devoted to investigate the seasonal variability of CO_2 and its fluxes (Section 3.2); finally, we evaluate the relative contribution of advection, mixing, air-sea exchange and biological activity to the seasonal cycle of CO_2 in the mixed layer of Azores area (Section 3.3).

2. Database and Methods

Surface CO_2 data sets from 10 cruises were combined in this study, being part of the CAVASSOO (http://tracer.env.uea.ac.uk/e072/) and CARINA databases (http://www.ifm.uni-kiel.de/fb/fb2/ch/research/carina). Tracks are shown in Fig. 1 and details are listed in Table 1. As part of the EU CANIGO project the Meteor 37/2, Azores 1, and Azores 2 cruises were performed. The AMT-3 and AMT-7 cruises were carried out within the British AMT (Atlantic Meridional Transects) project. The cruises PS9411, PS9502, PS9503, ST9506 and ST9507 comprise measurements on board ships of opportunity. Cruise period, principal scientist and number of data used for this study are specified in Table 1.

Regarding the analysis of CO_2 fugacity (fCO_2), various air-sea equilibration methodologies were used. During the Meteor 37/2 and Azores 1 cruises fCO_2 was determined with a system designed at the Instituto de Investigaciones Marinas,

similar to the one developed at the University of Kiel by Körtzinger *et al.* (1996). During the Azores 2 cruise fCO_2 was determined using a flow system similar to the one designed by Wanninkhof and Thoning (1993) and developed by Frank J. Millero´s group at the University of Miami. During the AMT, PS and ST cruises fCO_2 measurements were directly obtained using an automated air-sea CO_2 equilibration system, fully described by Cooper *et al.* (1998). All systems using an infrared analyser for analysis were calibrated by measuring two different standard gases provided by NOAA-CMDL (Climate Monitoring and Diagnostics Laboratory, Boulder, Colorado, USA) and by the Instituto Meteorológico Nacional (Izaña, Tenerife, Spain) calibrated against NOAA primary standards. The zero was set by means of synthetic air without CO_2 and H_2O.

Total alkalinity (TA) was potentiometrically determined during the Meteor 37/2, Azores 1, and Azores 2 cruises by open-cell titration (Mintrop *et al.*, 2000), one end-point titration (Pérez and Fraga, 1987), and a closed cell titration with two separate systems in parallel (Millero *et al.*, 1993), respectively. During the Meteor 37/2 cruise an intercalibration exercise was made among the three-potentiometric systems for alkalinity determination. This exercise clearly showed that the alkalinity accuracy was better than 1 μmol kg^{-1} (Mintrop *et al.*, 2000). The relationship between TA and salinity for the 69 surface data was TA=62.56 S+102 (r^2 = 0.94; $p<0.001$), with an estimated error of ±3.1 μmol.kg^{-1} (Fig. 2).

Total inorganic carbon (C_T) was calculated from fCO_2 and TA using the thermodynamic equations of the carbonate system with the dissociation constants of Mehrbach *et al.* (1973). Recently, Lee *et al.* (2000) and Lueker *et al.* (2000) have confirmed that the CO_2 constants by Merhbrach *et al.* (1973) are the most suitable for calculating C_T from TA and fCO_2. Besides, fCO_2 normalized to 25ºC –hereinafter

$fCO_2(25)$– was calculated at 25ºC from C_T and TA. This $fCO_2(25)$ variable is thermodynamically independent to the temperature and closely correlated with pH and C_T/TA.

Monthly average data for wind, sea surface temperature (SST), surface salinity (SSS), mixed layer depth (MLD), net heat flux (hereinafter heat flux) and evaporation less precipitation and runoff (EPR) for 1998 and the four first months of 1999 (28 months in total) were provided by B. Bernier and J.-M. Molines (Laboratoire Ecoulements Geophysique et Industriel de Grenoble, France), and used to establish the seasonal cycle in the Azores area. The region within 30-38ºN and 10-35ºW was divided into 9060 pixels of 8.4'x10.2'. The model data come from an Ocean General Circulation Model (OGCM), initialized from Reynaud *et al.* (1998) salinity and temperature climatology, spun up for 8 years by a climatological daily forcing. Then from 1979 to 2002, the model has been forced by daily atmospheric fluxes (heat, fresh water and wind stresses) from the ECMWF model. The data used in this study are monthly averages from this run.

The air-sea CO_2 exchange (mmol m^{-2} d^{-1}) was calculated using the equation:

$$FCO_2 = 0.24\ k\ S\ (fCO_{2air} - fCO_{2sea}) \quad (1)$$

where k is the transfer velocity (cm.h^{-1}), S is CO_2 seawater solubility (mol.kg^{-1}.atm^{-1}), fCO_{2sea} is surface ocean CO_2 fugacity, fCO_{2air} is atmospheric CO_2 fugacity (both in μatm) and 0.24 is an unit conversion factor. Seawater CO_2 solubility is calculated from Weiss (1974). Positive value indicates air to sea flux.

The impact of wind speed on the transfer velocity, k, was calculated using the equation ($k = 0.39\ u^2\ (Sc/660)^{-1/2}$) given by Wanninkhof (1992); u is the wind speed (m s^{-1}) and Sc is the Schmidt number calculated from its relation with temperature according to the polynomial fit given by Wanninkhof (1992).

3. Results and Discussion

3.1. Surface distributions in the Azores area.

Previous to any explanation of the seasonal CO_2 variability it is worthwhile to describe the main physical spatial features and fCO_2 distribution in the Azores area.

The Azores 1 cruise (August 1998) covered the widest area within this region and was chosen as representative for the typical spatial variability. The sea surface salinity and temperature (Fig. 3a, b) distribution is related to the position of the Azores Current (Pérez *et al.*, 2003) penetrating from the west with high temperature (>26ºC) and low salinity (<36.6). SST presents a strong eastward decreasing gradient. A slight north-south gradient is also noted, with higher temperatures north of about 33ºN. Similarly, SSS (Fig. 3a) increases also eastwards but in a smaller range than in the north-south direction. More saline surface waters are found south of the 32º-33ºN latitudinal band.

The surface *in situ* fCO_2 pattern (Fig. 3c) resembles the salinity distribution. Highest fCO_2 concentrations (>395 µatm) at the west are distinguishable from low values (<380 µatm) at the east. In the north-south direction lower differences are found, with slightly higher fCO_2 northwards. Although the thermodynamic effect of $fCO_2(25)$ was removed, the signal of chemical properties of the water masses remains on the $fCO_2(25)$. Hence, the surface distribution of $fCO_2(25)$ (Fig. 3d) matched well with SST, showing a remarkable westward decreasing gradient. The lowest $fCO_2(25)$ values (<380 µatm) were found west of 31º-32ºW associated with warmer waters (>26ºC), whereas the highest $fCO_2(25)$ (>400 µatm) values were related to waters colder than 24ºC. The west-east gradient is combined with a slight north-south gradient, with lowest $fCO_2(25)$ and highest SST northwards.

3.2. Seasonal variability of the surface CO_2.

The CO_2 seasonal cycle was assessed analysing our set of 10 cruises carried out at different months (Fig. 1 and Table 1) in the Azores region. In order to study the CO_2 seasonal cycle, fCO_2 measurements made during different years were corrected or normalised for the annual increase of atmospheric CO_2, and thus, referred to the common year 1998. The fCO_2 data have been corrected to 1998 using the annual rate of CO_2 surface water increase given by Takahashi *et al.* (1997) and González-Dávila *et al.* (2003) (1.3 μatm y^{-1}), which is consistent with the atmospheric rate. Surface waters in subtropical gyres mix vertically at slow rates with subsurface waters due to the presence of strong stratification at the base of the winter–mixed layer. Therefore, surface waters have a long time to equilibrate with the atmosphere (Takahashi *et al.*, 1997, 2002). Thus, the fCO_2 in these warm waters follow the increasing trend of atmospheric CO_2 as demonstrated by Inoue *et al.* (1995), Feely *et al.* (1999), and Bates (2002). Table 1 includes the normalising corrections for the fCO2 measurements.

The whole data set for surface CO2 normalized to 25ºC has also been corrected for the surface fresh water flux, this is, normalized to a constant salinity equal to 36.7, $fCO_2(25)_{36.7}$, which is calculated from a constant TA value and normalized CT (CT·36.7/salinity) from each sample using the dissociation constants by Mehrbach et al. (1973). In order to study the seasonal evolution of $fCO_2(25)_{36.7}$ we have plotted the whole data set against temperature within a field of fCO_2 isolines. This field has been obtained from constant salinity (36.7) and TA (2400 μmol kg^{-1}) values varying temperature (15º to 28ºC) and pHSWS (7.925 to 8.130) to obtain the in situ fCO_2 values. To match the in situ fCO_2 lines with the $fCO_2(25)_{36.7}$ data represented a unit conversion is done in order to easily observe the spatial and

temporal changes in the *in situ* fCO_2. Consequently, we can examine, on one hand as the distribution of *in situ* fCO_2 for each month is rather homogeneous showing the $fCO_2(25)_{36.7}$ values between at least two isolines (spatial changes), and on the other hand as the temperature increase the *in situ* fCO_2 became more and more higher (temporal changes), being in February (~ 320 µatm), reaching in August he highest values (~ 400 µatm). These changes are due to the variability of the surface water masses along the year.

So, in Figure 4, a clear relationship between $fCO_2(25)_{36.7}$ and SST for each cruise is discerned. Besides, as explained before, for each cruise the $fCO_2(25)_{36.7}$ values roughly follow the same *in situ* fCO_2 isoline (see also Fig.3C). So, the *in situ* fCO_2 changes are very small, indicating that the spatial distribution for each month is pretty homogeneous in fCO_2. As the seasonal cycle progresses, the set of cruises data change *in situ* fCO_2 isoline. Summer SST values (>26ºC) were associated with the highest *in situ* fCO_2 values (isoline ~400 µatm), while in winter, SST below 18ºC related with *in situ* fCO_2 isolines around 320 µatm. Fig. 4 also shows the annual fCO_2air isoline (355±2 µatm) for 1998 calculated at the temperature range from the xCO_2 obtained at the Izaña station (Tenerife, Spain). In this sense, two clusters of points are discerned: the sea-surface *in situ* fCO_2 values are lower than fCO_2air from November to June, and higher from June to November. In June and November the *in situ* fCO_2 seems to be practically in equilibrium with the atmospheric fCO_2 in the Azores area.

Consequently, the seasonal variation of $fCO_2(25)_{36.7}$ is related to SST. In the same way, $fCO_2(25)$ at real salinity also shows a seasonal variation with SST. The linear regression between $fCO_2(25)$ and SST for each cruise was of high significance in all cases with $r^2 > 0.73$ and $p<0.001$ (see Table 1). With the aim of establishing the

CO_2 seasonal cycle, $fCO_2(25)$ was adjusted against SST and month, the following expression was obtained:

$$fCO_2(25) = 431.40 - 31.391\ sin(2\pi/12\ (month+0.78)) - \\ - [13.225 - 2.127\ sin(2\pi/12\ (month - 2.86))]\ (SST-20) \quad (2)$$

Measured and calculated $fCO_2(25)$ are plotted in Fig. 5. The equation explains 86% of the total data variance. The slope of the measured versus calculated $fCO_2(25)$ is 1.014±0.003, and the mean difference between calculated and measured $fCO_2(25)$ is –3±7 µatm (n=20999). The small mean difference supports the consistency of our $fCO_2(25)$ fitted data.

The seasonal CO_2 cycle in the box of the Azores region was obtained using monthly average data of wind speed, and mixed layer temperature and salinity from 1998. The monthly $fCO_2(25)$ was calculated using equation (2) and monthly average SST. TA that was calculated by means of the equation given in Fig. 2. C_T was calculated from $fCO_2(25)$ and TA using the dissociation constants of Mehrbach *et al.* (1973). Seawater *in situ* fCO_2 (fCO_{2sea}) was also calculated from C_T and TA using monthly average SST data. The monthly atmospheric fCO_2 values were obtained at the Izaña station. Air-sea CO_2 fluxes (FCO_2) were calculated using equation (1) and the monthly average wind speed.

Even though there exists a spatial distribution with an eastward gradient in temperature, salinity and fCO_2 (Fig. 3) and some north south small variation, these spatial variations are of less significance in comparison with the seasonal variation (Fig. 4). To simplify the presentation of the seasonal cycle, the whole set of C_T, fCO_{2sea}, $fCO_2(25)$ and FCO_2 values was monthly averaged. Thus we obtain a monthly mean for each variable, spatially averaged in the studied Azores box area. In the next figures, the error for each average variable was estimated as the standard deviation

weighted by the number of data. These errors are very low, ranging from 0.011 for SST to 0.15 for $fCO_2(25)$, because of the large number of data (9060 pixels).

The seasonal variability of surface $fCO_2(25)$ resembles that of C_T (Fig. 6a). While, the seasonal cycle of fCO_{2sea} is opposite to C_T (Fig. 6b). The highest C_T (2070 μmol kg^{-1}) was found in April-May, decreasing abruptly (fCO_{2sea} increases) until September where it shows the lowest concentrations (2055 μmol kg^{-1}). Later, C_T increases until March-April where C_T reaches again higher concentrations (2069 μmol kg^{-1}). The C_T seasonal variation was only 15 μmol kg^{-1}, comparable to the range found in other oligotrophic regions, such as the North Pacific Subtropical Gyre (Weiss *et al.*, 1982; Winn *et al.*, 1994).

A strong seasonal variability is evident in fCO_{2sea}, with amplitude of 80 μatm (Fig. 6b). This variation is similar to the changes reported at the ESTOC site (60-80 μatm) from 1995-1997 (González-Dávila *et al.*, 2003) and at BATS site (80-100 μatm) from 1989 to 1993 (Bates *et al.*, 1996). This similarity could be caused by the advective connection between the Sargasso Sea Mode Waters in the western basin and modes of similar densities found in the eastern basin on the southern side of the Azores current (New *et al.*, 2001). The fCO_{2sea} annual cycle shows the characteristic minimum values of 315 μatm in winter (February) and maximum in summer (August) with values of 396 μatm. In comparison to this, fCO_{2air} is slightly higher in winter than in summer, but with amplitude of only 7 μatm. Consequently, surface water in the Azores area was CO_2 undersaturated from November to June and oversaturated from July to October. In general, FCO_2 along the year matched quite well the fCO_{2sea} distribution, showing some differences between January to March due to the wind effect. On the annual scale, the region acted as a CO_2 sink at a rate of 0.17 ±2.2 mmol m^{-2} d^{-1}. The maximum outgassing rate was obtained in August 1998

(3.84 mmol m^{-2} d^{-1}) and the maximum uptaking rate was in February 1999 (5.45 mmol m^{-2} d^{-1}). This uptake rate obtained in February 1999 is 4 times higher than that in February 1998, as wind speed in February 1999 was twice as high as in 1998.

A plot of the annual cycle of average fCO_{2sea} as a function of average SST for the Azores area is shown in Fig. 7 as an ellipsoid. Starting from fCO_{2sea} value of to 316 µatm at a temperature of 17.5ºC (March). The temperature increase at constant C_T of 2066 µmol kg^{-1} (see Fig. 6a) would thermodynamically lead to a fCO_2 increase of 15.4 µatm per ºC (dashed line in Fig. 7). So if only thermodynamical processes were active, it would be expected that fCO_2 changes would follow that line as from March to May. However, between June to August, the observed slope is lower than expected (12.5 µatm per ºC), likely as a consequence of a C_T decrease first by biological activity and afterwards by CO_2 outflux (Fig. 6a, b).

The starting conditions during the cooling period, i.e. from October onwards, are different, with a lower starting C_T concentration (2054 µmol kg^{-1}, Fig. 6a) at a temperature of 23.5ºC. So, the corresponding thermodynamical fCO_2 *vs.* SST slope would be 14.4 µatm per ºC (dashed-dot line in Fig. 7). From September to November the variation of fCO_2 indeed followed this slope. However, from November to February, fCO_2 *vs.* SST exhibited a smaller slope (8.8 µatm per ºC) as a consequence of C_T increase (Fig. 6a), probably due to advection and/or winter mixing. Similar fCO_{2sea}–SST relationships showing a seasonal change in the slopes were obtained by Bates *et al.* (1996) and Lefèvre and Taylor (2002) in the Atlantic gyres.

The FCO_2 values computed here are subject to three sources of error, the estimation of fCO_2, wind speed variations and the formulation of the gas transfer coefficient. The $fCO_2(25)$ was computed as a function of temperature (eq. 2) with an error of ±7 µatm. We use one standard deviation of ±2 m s^{-1} as wind speed error.

Normally distributed random perturbations of these errors (±7 µatm and ±2 m s^{-1}) were applied to the FCO_2 estimate, producing an error of ±0.024 mmol m^{-2} d^{-1} (~15%) due to the $fCO_2(25)$ and ±0.008 mmol m^{-2} d^{-1} (~5%) owing to the wind. These errors were estimated as the standard deviations of the FCO_2 mean generated by the perturbations. The FCO_2 errors using the perturbation analysis are very low due to the averaging effect acting on the independent errors in our large database that produces a considerable decrease of the real errors (Matsukawa and Suzuki, 1985). The other source of error in the FCO_2 estimate depends on the choice of the air-sea CO_2 gas transfer coefficient. We have used the Wanninkhof (1992) formulation obtaining an annual average of 0.17 mmol m^{-2} d^{-1} (0.06 mol m^{-2} yr^{-1}). The errors resulting from the use of other formulations have a systematic nature (Takahashi *et al.*, 1997). We have also made estimates of FCO_2 using the Liss and Merlivat (1986) and the Tans *et al.* (1990) exchange coefficients. The average CO_2 influxes were 0.09 and 0.19 mmol m^{-2} d^{-1}, respectively, which is 49% lower or 13% higher, respectively, than the mean FCO_2 value obtained with the Wanninkhof (1992) formulation.

This estimation of FCO_2 using different formulations is useful in order to compare our results with those from other authors. Takahashi *et al.* (1999) estimated a net FCO_2 influx ranging between 0 and 1 mol m^{-2} y^{-1} using the CO_2 gas transfer coefficient of Wanninkhof (1992) for the Azores area and the year 1995. Our net annual FCO_2 for 1998 is within this range.

The Azores area ($2.25 \cdot 10^{12}$ m^2) acted as a sink on the annual scale absorbing 0.004 Pg C yr^{-1} (0.38 mmol m^{-2} d^{-1}), as a result of the net influx of 0.102 Pg C yr^{-1} (10.3 mmol m^{-2} d^{-1}) from December to May, exceeding the net outflux of 0.098 Pg C yr^{-1}(9.9mmol m^{-2} d^{-1}) from June to November. These fluxes were calculated for the

year 1998 (see Table 2). Nevertheless at the light of the results observed in Fig. 6, with higher fluxes in February 1999 due to the increase in wind speed, significant FCO_2 interannual variability can be expected. In this sense, for the area comprised between 34º-38ºN and 10º-25ºW, we obtained air to sea flux $4.0 \cdot 10^{12}$ gC $y^{-1} \approx 1.4$ mmol m^{-2} d^{-1} (see Table 2), which is lower compared to $6.1 \cdot 10^{12}$ gC $y^{-1} \approx 2.1$ mmol m^{-2} d^{-1} for a reference year 1995 (Takahashi, personal communication and Takahashi et al., 1999). However if we take the period February 1998–January 1999, the influx for these area is higher ($10.5 \cdot 10^{12}$ gC $y^{-1} \approx 3.6$ mmol m^{-2} d^{-1}).

Several spatial patterns can be identified both during the outgassing and the ingassing periods. Maximum annual uptake values ($13 \cdot 10^{12}$ gC yr^{-1}) were obtained in the latitude band 36º-38ºN, minimum annual uptake values of $2.6 \cdot 10^{12}$ gC yr^{-1} were calculated for the latitude band 34º-36ºN. Between 32ºN and 34ºN, where the subtropical front, closely related to the position of the Azores Current, is more intense, the net annual uptake of CO_2 is low (~$2 \cdot 10^{12}$ gC yr^{-1}) west of 25ºW, acting as source ($5.4 \cdot 10^{12}$ gC yr^{-1}) east of 25ºW. Further south (latitude band 30-32ºN), the zone annually acts as a net source ($8.4 \cdot 10^{12}$ gC yr^{-1}). Annually, in all bands of latitude, CO_2 influx (outflux) is decreasing (increasing) eastwards (see Table 2).

In general, the monthly spatial distribution of the CO_2 influxes (outfluxes) presented the same spatial trend, with a southeastwards decrease (increase). There were exceptions in March, April and May where the trend of the CO_2 influx is decreasing northwestwards, due to a reduction of the trade wind intensity. Likewise, from July to October, due to wind modulation, the highest CO_2 sources appeared at the south of the studied zone, decreasing northwestwards. The lowest and uniform CO_2 fluxes for the whole area were in June (source) and November (uptake).

3.3. Role of the physical and biological processes in the CO_2 seasonal cycle

The rate of change of inorganic carbon (ΔC_T) in the mixed layer of the Azores box previously defined (30º-38ºN; 10º-35ºW) can be expressed as the sum of the different physical and biological processes that take place:

$$\Delta C_T = FCO_2 + \Delta C_{ADV} + \Delta C_{MIX} + \Delta C_{BIO} \quad (3)$$

ΔC_T is the total carbon rate of change in the mixed layer calculated as:

$$\Delta C_T = \frac{\delta(\rho \cdot C_{ML})}{\delta t} \cdot D \quad (4)$$

where C_{ML} is the C_T in the mixed layer; ρ is the seawater density; D is the mixed layer depth in metres; t is time in days.

FCO_2 is the variation of C_T due to the air-sea exchange of CO_2 between atmosphere and ocean, ΔC_{ADV} is the variation of carbon owing to advection, ΔC_{MIX} is the variation of carbon due to the mixing with the lower layer, and ΔC_{BIO} stands for the variation of carbon due to biological activity.

Conservation equations for salinity and temperature within the mixed layer of our Azores box are applied to calculate advection and mixing. According to the general scheme of circulation in the zone (Schmitz, 1996; Pingree, 2002) there is an advection of waters eastwards that leaves the box southwards. The mixing occurs with waters located below the mixed layer.

The following system of conservation equations are formulated for salinity and temperature:

$$Q_{ADV} \cdot (S_W - S_S) + Q_{MIX}(S_{LL} - S_{ML}) + (EPR) \cdot S_S = \frac{\delta(V \cdot S_{ML})}{\delta t}$$

$$Q_{ADV} \cdot (T_W - T_S) + Q_{MIX}(T_{LL} - T_{ML}) + (EPR) \cdot T_S + Heat = \frac{\delta(V \cdot T_{ML})}{\delta t} \quad (5)$$

where Q_{ADV} is the horizontal advection flow into the box; Q_{MIX} is the vertical mixing flow –both expressed in $m^3\ day^{-1}$– that crosses the *MLD*; S_W and S_S and T_W and T_S are the salinity and temperature values in the west and south walls of the box; S_{ML} and T_{ML} are monthly average salinity and temperature of the mixed layer. S_{LL} and T_{LL} stand for salinity and temperature in the low layer situated just below the mixed layer. We have considered 180 metres as the stationary deep layer (*DL*) that mixes with the low layer for the whole annual cycle with S_{DL} = 36.43 and T_{DL} = 16.4ºC according to Arhan *et al.* (1994). The low layer varies with time and is taken as $1.5 \cdot MLD$. S_{LL} and T_{LL} for each month were calculated by linear interpolation between S_{ML} and T_{ML} at the $0.5 \cdot MLD$ and S_{DL} and T_{DL} at 180 m. *V* stands for the box volume ($V = A \cdot MLD$) expressed in m^3, being A the area of the box ($2.25 \cdot 10^{12}\ m^2$).

Once we have the flows of advection (Q_{ADV}) and mixing (Q_{MIX}) for each month we can calculate the rate of change of C_T due to these processes, ΔC_{ADV} and ΔC_{MIX}, according to the following expressions:

$$\Delta C_{ADV} = \rho \cdot Q_{ADV} \cdot (C_W - C_S) / A$$

$$\Delta C_{MIX} = \rho \cdot Q_{MIX} \cdot (C_{LL} - C_{ML}) / A \qquad (6)$$

where C_W and C_S are the C_T in the west and south walls of the box; C_{ML} is the C_T in the mixed layer; C_{LL} stands for C_T in the low layer situated just below the mixed layer. The C_{LL} was calculated from TA_{LL} and $fCO_2(25)_{LL}$ using the Mehrbach *et al.* (1973) constants. TA_{LL} was computed for each month as a function of S_{LL} using the equation given in Fig. 2, and $fCO_2(25)_{LL}$ was determined as a function of T_{LL} for each month, using equation (2).

Knowing all terms of equation (3) ΔC_{BIO} can be calculated by subtraction. All the rates are expressed in mmol m^{-2} d^{-1} and in all cases positive (negative) values indicate an increase (decrease) of carbon within the box.

Fig. 8a shows the evolution of ΔC_{ADV}, ΔC_{MIX} and ΔC_{BIO} during 1998, the coupling between them is obvious. More than 80% of the total variability of ΔC_{BIO} can be explained by multiple linear regression (r^2=0.81; n=15; p<0.001) with ΔC_{MIX} and ΔC_{ADV}. So, when ΔC_{MIX} increases in the mixed layer as a consequence of an injection of C_T from the lower level, the biological activity (a shorter scale than one month) developed by the phytoplankton in the mixed layer produces a decrease in ΔC_{BIO}. The C_T supplied by advection increases ΔC_{MIX} to support the biological activity in practically all year. When the ΔC_{MIX} is not fully compensated by the biological activity (e.g. January 1999), there is a loss of C_T by advection (negative ΔC_{ADV} values in Fig. 8a).

The net average value of ΔC_{ADV} obtained in this study was 1.7 mmol m^{-2} d^{-1}. Williams and Follows (1998) have estimated the horizontal transfer of nutrients in the North Atlantic Ocean. They found that this horizontal transfer on the northern flank of the subtropical gyre, provides a source of nitrate from 0.06 to 0.12 mol m^{-2} yr^{-1} which corresponds to 1.1–2.2 mmol m^{-2} d^{-1} of carbon assuming a C:N = 106:16 according to Redfield *et al.* (1963). Our average ΔC_{ADV} is within the range obtained by these authors.

The ΔC_{BIO} represents the net community production rate in the mixed layer of the Azores area. Our ΔC_{BIO} values can be validated with direct primary production data reported by different authors (rings in Fig. 8a). The rates of primary production obtained by several authors (Frazel and Berberian, 1990; Jochem and Zeitzschel, 1993; Fernández and Pingree, 1996; Marañón *et al.*, 2000; Mouriño *et al.*, 2001;

Lorenzo *et al.*, 2004) were estimated by ^{14}C inoculation, which can be assimilated as gross or total primary production. We have estimated a ratio between new and total primary production (*f*–ratio) of 0.30 applying an empirical equation of general applicability given by Tremblay *et al.* (1997) as a function of total production. We have taken the annual primary production (10 mol m^{-2} yr^{-1}) obtained by Sathyendranath *et al.* (1995) on the flanks of the North Atlantic Subtropical Gyre using remotely sensed chlorophyll. This *f*–ratio is in agreement with the 0.26 given by Eppley and Peterson (1979). Thus, all gross productions quoted in the bibliography were converted to new production using an *f*-ratio of 0.30.

As observed in Fig. 8a, most measured net production values taken from different field studies (Frazel and Berberian, 1990; Jochem and Zeitzschel, 1993; Fernández and Pingree, 1996; Marañón *et al.*, 2000; Mouriño *et al.*, 2001; Lorenzo *et al.*, 2003) follow the evolution of the net production calculated with the proposed approach. The difference between the measured and calculated values ranges between 1 and 3.2 mmol m^{-2} d^{-1}. Only in December the reported and here-calculated productions exhibit higher difference. The net production estimated in this study is referred to 1998. Just two measurements were done in 1998, those in August from Mouriño *et al.* (2001) and Lorenzo *et al.* (2004) both measured during the Azores 1 cruise and were 10 and 8.7 mmol m^{-2} d^{-1}, respectively, in good agreement with our estimated value (11.4 mmol m^{-2} d^{-1}). The other production data reported by different authors were obtained during cruises carried out between 1989 and 1999. Therefore, it is likely that the productions with higher differences are affected by different environmental conditions for the year of the sampling, provoking higher or lower productions than expected for 1998.

On the other hand, Sathyendranath *et al.* (1995) estimate that the annual primary production reaches 10 mol m^{-2} yr^{-1} over the flanks of the subtropical gyre using remotely sensed chlorophyll. Assuming the *f*-ratio of 0.30 the new production is 8.2 $mmol.m^{-2}.d^{-1}$, which is in good agreement with our net annual average of ΔC_{BIO} (−8.9 ±4.6 mmol m^{-2} d^{-1}). The good agreement between ΔC_{BIO} and the primary production given by several authors, as well as the accordance of ΔC_{ADV} with the estimates made by Williams and Follows (1998) support the calculated ΔC_{MIX} values.

The amplitude of ΔC_{ADV} (Fig. 8a) and ΔC_T and FCO_2 (Fig. 8b) are much smaller than the amplitude of ΔC_{MIX} and ΔC_{BIO} (Fig. 8a). The annual average of ΔC_T is 0.8 ±2.5 mmol m^{-2} d^{-1}. So, the contribution of the air-sea exchange (FCO_2= 0.17 mmol m^{-2} d^{-1}) and the advection (ΔC_{ADV}= 1.7 mmol m^{-2} d^{-1}) on the total CO_2 mass balance is very small. The net annual average of the mixing (ΔC_{MIX}= 7.8 mmol m^{-2} d^{-1}) and biological activity (ΔC_{BIO}= −8.9 mmol m^{-2} d^{-1}) are the most important contributors to the CO_2 variation in the mixed layer.

The negligible contribution of FCO_2 and ΔC_{ADV}, and the high disproportionate contribution of ΔC_{MIX} and ΔC_{BIO} to the ΔC_T variability is easy to understand, as the processes, ΔC_{MIX} and ΔC_{BIO}, together with ΔC_{ADV} are coupled as already mentioned. To assess the rates of change of ΔC_T and FCO_2 in the mixed layer, it is essential to consider the net balance between the biological response to the entrainment of C_T and nutrients by mixing and in minor proportions by advection. This photosynthetic response to the nutrients and C_T inputs is faster than the monthly scale used here. So, these three-coupled processes −ΔC_{ADV}, ΔC_{MIX} and ΔC_{BIO}− have been combined as ΔC_{AMB}. This term represents the net effect of the biological community in the water column in response the vertical mixing, which is supported

by the vertical gradient generated by degradation of biogenic debris produced in the mixed layer and transported by gravitational settling to deeper layers.

The evolution of ΔC_T, FCO_2 and ΔC_{AMB} is shown in Fig. 8b. Three different scenarios can be distinguished. In the first one between February and June MLD decreases as SST increases, the variation of C_T is very low (0.03 ± 0.36 mmol m^{-2} d^{-1}). There is an excess of CO_2 uptake by biological processes over the input by mixing and advection from February to May (see Fig. 8a). This excess of CO_2 uptake favours the entry of CO_2 through the air-sea interface, in such way that the net CO_2 uptake in the MLD is balanced with the air-sea CO_2 exchange. In the second scenario between July and October the MLD becomes shallower due to heating, which favours the emission of CO_2 through the air-sea interface. This loss of CO_2 surpasses the C_T supplied by mixing and advection over the biological uptake meaning a C_T decrease. Basically the summer heating in a reduced mixed layer drives the loss of CO_2, which is moderated by the positive balance of ΔC_{AMB}. In the third scenario (November-January), the MLD increases and waters get cooler, C_T concentrations increase by mixing and mineralization of organic matter. The entry of CO_2 through the air-sea interface increases gradually reaching a maximum in February, when the MLD increases and the biological activity becomes important.

After establishing the concept of net biological production in the water masses (ΔC_{AMB}) due to the advection and mixing processes, we need to re-evaluate the contribution of the physical processes and biological activity because, as we can see in Fig. 8, the amplitude of the different rates of change have decreased from 32 mmol m^{-2} d^{-1} to 11 mmol m^{-2} d^{-1}. For this purpose, a multiple linear regression of ΔC_T with temperature, wind speed and ΔC_{AMB} ($r^2=0.71$; $n=15$; $p<0.001$) allows us to estimate the effect of physical and biological processes, resulting that 46% of the

ΔC_T mass balance is due to the ΔC_{AMB} contribution, 12% due to wind and 42% to temperature. Therefore, we can conclude for the Azores area that the contribution of the physical processes is higher than the biological ones, although both processes are fairly balanced.

4. Summary and Conclusions

Given the relevance of the subtropical gyres as convergence zones favouring the accumulation of CO_2 in the ocean, this study has been made with the aim of assessing the seasonal variability of the sea surface CO_2 in the Azores area, evaluating the physical and biological processes affecting its rates of change in the mixed layer.

The seasonal sea-surface cycle of CO_2 was evaluated modelling the CO_2 fugacity with temperature and month using a data set of 10 cruises carried out in the Azores area (30º-38ºN; 10-35ºW). Monthly variables of the carbon system and CO_2 air-sea fluxes were calculated using the algorithm obtained and monthly average data for wind speed and mixed layer temperature and salinity.

The air-sea CO_2 fluxes obtained demonstrate that the Azores area acts as a weak sink of CO_2 with an uptake of 0.004 Pg C yr^{-1}. Such sink represents around 0.23% of the net oceanic CO_2 sink (1.7±0.7 Pg C yr^{-1} in the 1990s) reported by the IPCC (2001).

The role of the physical and biological processes in the CO_2 seasonal cycle was monthly assessed to investigate the contribution of each process. The rate of change of the total carbon in the mixed layer can be expressed as the sum of the CO_2 air-sea exchange and variations due to advection, mixing with the lower layer, and biological activity. Advection and mixing in our Azores box were estimated from

conservative equations for salinity and temperature. Once these flows were obtained, the corresponding rates of changes due to the different factors affecting the CO_2 mass balance were estimated. Biological activity was also inferred and validated by comparison with primary production field data reported by several authors.

The most important contributors to the average mass balance of CO_2 (0.8 mmol m^{-2} d^{-1}) in the mixed layer are mixing (7.8 mmol m^{-2} d^{-1}) and biological activity (-8.9 mmol m^{-2} d^{-1}). Conversely, the contributions of the air-sea exchange (0.17 mmol m^{-2} d^{-1}) and the advection (1.7 mmol m^{-2} d^{-1}) are very small.

Taking into account that the biological activity in the mixed layer (ΔC_{BIO}) is coupled with ΔC_{ADV} that ΔC_{MIX} that introduce C_T in the mixed layer, we have combined the three physical and biological processes obtaining the variable ΔC_{AMB} that represents the net effect of biological production in the water column. The effect of the physical processes (temperature and wind) and the net production (ΔC_{AMB}) on the total CO_2 mass balance was then re-evaluated, resulting that 42% is due to the temperature, 12% by the wind action and 46% by the net balance of photosynthetic activity due to the injection of nutrients from the deeper layer and horizontal advection.

Acknowledgements

This work was supported by the EU CAVASSOO project (EVK2-2000-00088) and EU CANIGO project (MAS3-CT96-0060). M. Álvarez was funded by the European Union under a Global Change I3P postdoctoral contract. The authors wish to thank all the participants in the 10 cruises and masters, officers and crew of the research vessels “Meteor”, “Hespérides”, “James Clark Ross”, and ships of opportunity “Prince of Seas” and “St. Helena”. We are very grateful to Jean-Marc

Molines and Bernard Barnier from the Laboratoire Ecoulements Geophysique et Industriel of Grenoble for providing the monthly average data in the format required. Special thanks to Jean-Marc Molines for his explanations about the former data and to Ramón Ramos and Emilio Cuevas from the Instituto Meteorológico Nacional of Izaña for the calibration of CO_2 standards and to provide atmospheric xCO_2 data. We are also very grateful to Rik Wanninkhof and the other anonymous reviewer for the carefully review of this manuscript.

References

Arhan, M., Colin de Verdière, A., Mémery, L., 1994. The Eastern Boundary of the Subtropical North Atlantic. Journal of Physical Oceanography, 24, 1296-1316.

Bates, N.R., Michaels, A.F., Knap, A.H., 1996. Seasonal and interannual variability of oceanic carbon dioxide species at the U.S. JGOFS Bermuda Atlantic time-series study (BATS) site. Deep-Sea Res. II, 43(2-3), 347-383.

Bates, N.R. Pequignet, A.C., Rodney J. Johnson, R.J., Gruber, N., 2002. .A short-term sink for atmospheric CO2 in subtropical mode water of the North Atlantic Ocean. Nature, 420, 489-493.

Cooper, D.J., Watson, A.J., Ling, R.D., 1998. The seasonal cycle of pCO_2 along a North Atlantic shipping route (U.K. to Jamaica). Mar. Chem., 60, 147-164.

Eppley, R.W., Peterson, B.J., 1979. Particulate organic matter flux and planktonic new production in the deep ocean. Nature, 282, 677-680.

Fernández, E., Pingree, R.D., 1996. Coupling between physical and biological fields in the North Atlantic subtropical front southeast of the Azores. Deep-Sea Res. I, 43, 1369-1393.

Gould, W.J., 1985. Physical oceanography of the Azores front. Prog. Oceanog., 14, 167-190.

Feely, R.A., Wanninkhof, R., Takahashi, T., Tans, P., 1999. Influence of El Niño on the equatorial Pacific contribution to atmospheric CO2 accumulation. Nature 398, 597-601.

Follows, M.J., Williams, R.G., Marshall, J.C., 1996. The solubility pump of carbon in the subtropical gyre of the North Atlantic. J. Mar. Res., 54, 605-630.

Frazel, D.W., Berberian, G., 1990. Distributions of chlorophyll and primary productivity in relation to water column structure in the eastern North Atlantic Ocean. Global Biogeochem. Cycles 4, 241-251.

González-Dávila, M., J.M. Santana-Casiano, J.M., Rueda, M.J., Llinás, O., González-Dávila, E.F., 2003. Seasonal and interannual variability of sea-surface carbon dioxide species at the European Station for Time Series in the Ocean at the Canary Islands (ESTOC) between 1996 and 2000. Global Biogeochemical Cycles, 17(3), 1076, doi:10.1029/2002GB001993.

Inoue, H.Y., Matsueda, H., Ishii, M., Fushimi, K., Hirota, M., Asanuma, I., Takasugi,

Y., 1995. Long-term trend of the partial pressure of carbon dioxide (pCO2) in surface waters of the western North Pacific, 1984-1993. Tellus 47B, 391-413.

IPCC, Intergovernmental Panel on Climate Change, Climate Change 2001: The Scientific Basis, Cambridge University Press, 881 p., 2001.

Jochem F.J., Zeitzschel, B., 1993. Productivity regime and phytoplankton size structure in the tropical North Atlantic in spring 1989. Deep-Sea Res.II, 40(1/2), 495-519.

Käse, R.H., Siedler, G., 1982. Meandering of the subtropical front, south-east of Azores. Nature, 300, 245-246.

Käse, R.H., Zenk, W., Sanford, T.B., Hiller, W., 1985. Currents, fronts and eddy fluxes in the Canary basin. Prog. Oceanog., 14, 231-257.

Klein, B., Siedler, G., 1989. On the origin of the Azores current. J. Geophys. Res., 94, 6159-6168.

Körtzinger, A., Thomas, H., Schneider, B., Gronau, N., Mintrop, L., Duinker, J.C., 1996. At-sea intercomparison of two newly esigned underway pCO_2 system - Encouraging results. Mar.Chem., 52, 133-145.

Lefèvre, N., Taylor, A., 2002. Estimating pCO_2 from sea surface temperatures in the Atlantic gyres. Deep Sea Research I, 49, 539-554.

Liss, P.S., Merlivat, L., 1986. Air-sea gas exchange rates:Introduction and synthesis in: The role of air-sea exchange in geochemical cycling...Buat-Ménard,P.D. Reidel Publishing Company., 113-127.

Lee, K., Millero, F.J., Byrne, R.H., Feely, R.A., Wanninkhof, R., 2000. The recommended dissociation constants for carbonic acid in seawater. Geophysical Reseach Letters, 27(2), 229-232.

Lorenzo, L.M., Figueiras, F.G., Tilstone, G.H., Arbones, B., Mirón, I., 2004. Photosynthesis and light regime in the Azores Front region during summer. Are light-saturated computations of primary production sufficient?. Deep-Sea Res. I, 51: 1229–1244.

Lueker, T.J., Dickson, A.G., Keeling, C.D., 2000. Ocean pCO_2 calculated from dissolved inorganic carbon, alkalinity and equations for K1 and K2: validations based on laboratory measurements of CO2 in gas and seawater at equilibrium. Mar. Chem., 70, 105-119.

Marañón, E., Holligan, P.M., Varela, M., Mouriño, B., Bale, A.J., 2000. Basin-scale variability of phytoplankton biomass, production and growth in the Atlantic Ocean. Deep-Sea Research II, 47(5), 825-857.

Marshall, J.C., Nurser, A.J.G., Williams, R.G., 1993. Inferring the subduction rate and period over North Atlantic, J. Phys. Oceanogr., 23, 1315–1329

Matsukawa, Y., Suzuki, T., 1985. Box model analysis of hydrographic behaviour of nitrogen and phosphorus in a eutrophic estuary. J. Oceanogr. Soc. Jpn. 41, 407–426.

Mehrbach, C., Culberson, C.H., Hawley, J.E., Pytkowicz, R.M., 1973. Measurement of the apparent dissociation constants of carbonic acid in seawater at atmospheric pressure. Limnology and Oceanography, 18, 897-907.

Millero, F.J., Zhang, J-Z., Lee, K., Campbell, D.M., 1993. Titration alkalinity of seawater. Mar. Chem., 44, 143-152.

Mintrop, L., Pérez, F.F., González-Dávila, M., Santana-Casiano, J.M., Körtzinger, A., 2000. Alkalinity determination by potentiometry – intercalibration using three different methods. Ciencias Marinas, 26, 23-37.

Mouriño, B., Fernández, E., Serret, P., Harbour, D., Sinha, B., Pingree, R., 2001. Variability and seasonality of physical and biological fields at the Great Meteor Tablemount (subtropical NE Atlantic). Oceanologica Acta, 24(2), 167-185.

New, A.L., Jia, Y., Coulibaly, M., Dengg, J., 2001. On the role of the Azores Current in the ventilation of the North Atlantic Ocean, Prog. Oceanogr., 48, 163–194.

Pérez, F.F., Fraga, F., 1987. A precise and rapid analytical procedure for alkalinity determination. Marine Chemistry, 21, 169-182.

Pérez, F.F., Gil-Coto, M., Ríos, A.F., 2003. Large and mesoscale variability of the water masses and the DCM the Azores Front. Journal Geophysical Research, 108 (C7) 10.1029/2000JC000360.

Pingree, R.D., 1997. The eastern subtropical gyre(North Atlantic):flow rings recirculations structure and subduction. J. Mar. Biol. Ass. U.K., 77, 573-624.

Pingree, R., 2002. Ocean structure and climate (Eastern North Atlantic): in situ measurement and remote sensing (altimeter). Journal Marine Biological Association U.K, 82, 681-707.

Pingree, R.D., Sinha, B., 1998. Dynamic topography (ERS-1/2 and seatruth) of Subtropical ring (Storm 0) in the Storm corridor (32-34ºN, Eastern basin, North Atlantic Ocean). J. Mar. Biol.. Ass. U.K., 78, 351-376.

Redfield, A.C., B.H. Ketchum and F.A. Richards. 1963. The influence of organisms on the composition of sea-water. pp.26-77. in M.N. Hill ed.The Sea. Vol.2, pp.554. John Wiley & Sons, New York.

Reynaud, T., P. Legrand, H. Mercier and B. Barnier. 1998. A new analysis of hydrographic data in the Atlantic and its application to inverse modelling study. Woce Newsletter 32:29-31.

Sathyendranath, S., Longhurst, R.S.A., Caverhill, C.M., Platt, T., 1995. Regionally and seasonally differentiated primary production in the North Atlantic. Deep-Sea Res. I, 42, 1773-1802.

Schmitt, R.W., Bogden, P.S., Dorman, C.L., 1989. Evaporation minus precipitation and density fluxes for the North Atlantic, J. Phys. Oceanogr., 19, 1208–1221.

Siedler, G., Kuhl, A., Zenk, W., 1987. The Madeira mode water, J. Phys. Oceanogr., 17, 1561–1970.

Schmitz, W.J., Jr., 1996. On the World Ocean Circulation: Volume I. Some Global Features/North Atlantic Circulation. Woods Hole Oceanographic Institutuion. Technical Report WHOI-96-03, 141 pp.

Stramma, L., 1984. Geostrophic transport in the Warm Water Sphere of eastern subtropical North Atlantic. J. Mar. Res., 42: 537-558.

Sy, A., 1988. Investigation of large-scale circulation patterns in the central North Atlantic: The North Atlantic Current, the Azores Current, and the Mediterranean water plume in the area of the Mid-Atlantic Ridge. Deep-Sea Res. I, 35, 383-413.

Takahashi, T., Feely, R.A., Weiss, R.F., Wanninkhof, R.H., Chipman, D.W., 1997. Global air- sea flux of CO_2 : An estimate based on measurements of sea-air pCO_2 difference. Proc.Nat.Acad.Sci., 94, 8292-8299.

Takahashi, T., Wanninkhof, R.H., Feely, R.A., Weiss, R.F., Chipman, D.W., Bates, N., Olafsson, J., Sabine, C., Sutherland, S.C., 1999. Net sea-air CO_2 flux over the global oceans: An improved estimate based on the sea-air pCO_2 difference. Proceedings of the 2nd International Symposium CO_2 in the Oceans, Tsukuba, CGER-I037-'99, 9-15.

Takahashi, T., S.C. Sutherland, C. Sweeney, A. Poisson, N. Metzl, B. Tilbrook, N. Bates, R. Wanninkhof, R.A. Feely, C. Sabine, J. Olafsson, Y. Nojiri. 2002. Glogal sea-air CO_2 flux based on climatological surface ocean pCO_2, and seasonal biological and temperature effects. Deep-Sea Res.II, 49, 1601-1622.

Tans, P.P., Fung, I.Y., Takahashi, T., 1990. Observational Constraints on the global atmospheric CO_2 budget. Sci., 247, 1431-1438.

Tremblay, J-E., Klein, B., Legendre, L., Rivkin, R.B., Therriault, J-C., 1997. Estimation of *f*-ratios in oceans based on phytoplankton size structure. Limnol. Oceanogr., 42, 595-601.

Wanninkhof, R., Thoning, K., 1993. Measurement of fugacity of CO_2 in surface water using continuous and discrete sampling methods. Mar. Chem., 44, 189-204.

Wanninkhof, R., 1992. Relationship between wind speed and gas exchange over the ocean. J. Geophys. Res., 97, 7,373-7,383.

Weiss, R.F., Jahnke, R.A., Keeling, C.D., 1982. Seasonal effects of temperature and salinity on the partial pressure of CO_2 in seawater. Nature, 300, 511-513.

Weiss, R.F., 1974. Carbon dioxide in water and seawater. The solubility of a non ideal gas. Mar. Chem., 2, 203-215.

Williams, R.G., Follows, M.J., 1998. The Ekman transfer of nutrients and maintenance of new production over the North Atlantic. Deep-Sea Research I, 45, 461-489.

Winn, C.D., Mackenzie, F.T., Carrillo, C.J., Sabine, C.L., Karl, D.M., 1994. Air-sea carbon dioxide exchange in the North Pacific Subtropical Gyre: implications for the global carbon budget. Global Biogeochemical Cycles, 8, 157-163.

Figure captions

Fig. 1. – Map of the sampled area and tracks of the 10 cruises. The year and month of each cruise are indicated. Further details in Table 1.

Fig. 2. – Relationship between surface total alkalinity and salinity.

Fig. 3. – Distribution of a) sea surface salinity (SSS), b) sea surface temperature (SST) in ºC, c) sea surface *in situ* fCO_2 in µatm, d) sea surface fCO_2 at 25ºC in µatm, during the Azores-1 cruise (August 1998). Grey dots stand for the cruise track.

Fig. 4.– Relationships between observational $fCO_2(25)$ at salinity 36.7 and sea surface temperature (ºC) on a theoretical *in situ* fCO_2 field at salinity 36.7 in surface waters for the 10 cruises indicated in Figure 5. The *in situ* fCO_2 isolines field has been created from constant salinity (36.7) and TA (2400 µmol kg^{-1}), and variable temperature (15º to 28ºC) and pHSWS at 25ºC (8.130 to 7.925), using the same dissociation constants of Mehrbach *et al.* (1973). Different symbols and colours identify the cruises: Meteor 37/2–blue open diamond; PS9502–red open triangle down; PS9503–green open circle; Azores 2–magenta open square; ST9506–orange open triangle up; ST9507–deep yellow open diamond; Azores 1–blue cross; AMT-3 –magenta X-shape; AMT-7–red open triangle up; PS9411–blue open circle. The doted line stands for atmospheric fCO_2.

Fig. 5. – Relationship between measured and calculated fCO_2 at 25ºC.

Fig. 6. – Average monthly evolution of a) sea surface $fCO_2(25)$(µatm) and C_T (µmol kg^{-1}), b) sea surface(fCO_{2sea}) and air (fCO_{2air}), both in µatm, and air-sea CO_2 fluxes (FCO_2 in mmol m^{-2} d^{-1}) for the Azores area. Positive fluxes indicate air to sea exchange.

Fig. 7.- Annual cycle of average sea surface fCO_{2sea} (µatm) versus SST (ºC) for the Azores area. The cycle starts in February 1998 and finished in March 1999 when the values of both variables (fCO_{2sea} and SST) are coincident with March 1998. The dashed line depicts the thermodynamical theoretical line for initial conditions in March (slope 15.4 µatm/ºC). Dash-dot line represents the thermodynamical theoretical line for initial conditions in October (slope 14.4 µatm/ºC).

Fig. 8. – a) Temporal evolution of the total inorganic carbon variation due to the biological processes ((ΔC_{BIO} black diamond), mixing with the lower layer (ΔC_{MIX} open diamond) and advection (ΔC_{ADV} black triangle) in the mixed layer of the defined Azores box. The evolution of the mixed layer depth (MLD) is also shown. B) Temporal evolution of the total inorganic carbon variation (ΔC_T), its contribution from the air-sea exchange (FCO_2), and the term ΔC_{AMB}, which combines the changes in C_T due to the biological activity, mixing and advection. Positive values mean an increase of carbon in the mixed layer. Units in mmol m^{-2} d^{-1} except the MLD in metres. Rings stand for new production values derived from experimental primary production values in the area converted to new production using an *f*-ratio equal to 0.3: JZ = Jockem and Zeitzschel, 1993; Mo = Mouriño *et al.*, 2001; FP = Fernández and Pingree, 1996; FB = Frazel and Berberian, 1990; Ma = Marañón *et al.*, 2000; L = Lorenzo *et al.*, 2004.

Table 1
Characteristics of the 10 cruises carried out in the Azores area sorted by time (year and month). The tracks and stations sampled in each cruise are represented in Figure 1. *Correct. fCO_2* is the correction made at the fCO_2 (μatm) of every cruise to refer to 1998. r^2 is the determination coefficient of the linear regression between $fCO_2(25)$ and SST for each cruise. N is the number of data.

Time [yymm]	Cruise	Vessel/Principal Scientist of fCO_2	*Correct.* fCO_2	r^2	N
9701	Meteor 37/2	Meteor / F.F. Pérez	+2	0.73	3795
9502	PS9502	Prince of seas / N. Lefèvre	+4	0.96	114
9503	PS9503	Prince of seas / N. Lefèvre	+4	0.96	123
9904	Azores 2	Hespérides / M.González Dávila	-1	0.75	10769
9506	ST9506	St. Helena / A.J. Watson, D.J.Cooper, N. Lefèvre	+4	0.90	260
9507	ST9507	St. Helena / A.J. Watson, D.J.Cooper, N. Lefèvre	+4	0.87	253
9808	Azores 1	Hespérides / F.F. Pérez	+0	0.86	5014
9609	AMT-3	James Clark Ross/N. Lefèvre	+3	0.76	140
9809	AMT-7	James Clark Ross/N. Lefèvre	+0	0.87	378
9411	PS9411	Prince of seas/A.J. Watson, D.J.Cooper, N. Lefèvre	+5	0.97	153
		Total			20999

Table 2

Monthly and mean annual net CO_2 flux over the Azores area (in 10^{12} g C·yr^{-1} across each 2º x 5º pixel area) computed for 1998 using the gas transfer coefficient (eq. 2) of Wanninkof (1992). Positive values air-sea flux, negative values sea-air flux.

Latitude	Longitude	1	2	3	4	5	6	7	8	9	10	11	12	Annual	
36º-38ºN	10º-15ºW	0.24	0.62	1.35	2.15	1.13	0.05	-1.41	-3.24	-0.84	-0.35	0.33	0.77	0.80	
	15º-20ºW	0.66	0.69	1.18	1.91	1.23	0.01	-1.02	-2.44	-0.69	-0.28	0.14	0.54	1.93	
	20º-25ºW	0.97	0.96	0.57	1.27	0.65	-0.03	-0.62	-0.83	-0.59	-0.26	0.06	0.74	2.89	
	25º-30ºW	1.58	1.30	0.44	0.49	0.15	-0.12	-0.38	-0.36	-0.51	-0.32	0.01	0.92	3.20	
	30º-35ºW	1.87	1.30	1.07	0.43	0.21	-0.20	-0.17	-0.10	-0.66	-0.79	0.01	1.27	4.24	13.06
34º-36ºN	10º-15ºW	0.48	0.42	1.61	1.82	0.89	-0.22	-1.92	-3.72	-1.19	-0.63	0.18	0.73	-1.55	
	15º-20ºW	0.39	0.30	1.46	1.51	0.80	-0.14	-1.52	-2.91	-0.71	-0.55	0.05	0.38	-0.94	
	20º-25ºW	0.85	0.51	1.24	1.01	0.47	-0.13	-1.07	-1.39	-0.37	-0.44	0.01	0.24	0.93	
	25º-30ºW	1.30	0.84	0.87	0.39	0.16	-0.12	-0.80	-0.59	-0.20	-0.36	-0.01	0.42	1.90	
	30º-35ºW	1.35	0.91	0.83	0.14	0.21	-0.09	-0.56	-0.21	-0.22	-0.60	0.00	0.46	2.22	2.56
32º-34ºN	10º-15ºW	1.02	0.52	1.82	2.28	0.70	-0.51	-2.33	-3.97	-1.57	-1.01	0.15	0.70	-2.20	
	15º-20ºW	0.30	0.34	1.56	1.65	0.50	-0.39	-1.98	-3.13	-0.95	-0.79	0.02	0.48	-2.39	
	20º-25ºW	0.49	0.42	1.51	1.26	0.34	-0.32	-1.58	-1.91	-0.59	-0.60	-0.01	0.23	-0.76	
	25º-30ºW	1.06	0.60	1.31	0.77	0.18	-0.26	-1.27	-0.95	-0.36	-0.42	-0.03	0.41	1.04	
	30º-35ºW	0.82	0.51	1.07	0.45	0.16	-0.18	-1.07	-0.40	-0.29	-0.48	-0.02	0.32	0.89	-3.42
30º-32ºN	10º-15ºW	0.97	0.71	1.84	2.77	0.66	-0.58	-2.34	-3.83	-1.67	-1.16	0.13	0.62	-1.88	
	15º-20ºW	0.50	0.27	1.74	1.80	0.29	-0.71	-2.44	-3.20	-1.30	-1.00	0.00	0.73	-3.32	
	20º-25ºW	0.45	0.35	1.73	1.64	0.25	-0.65	-2.28	-2.57	-1.01	-0.72	-0.02	0.52	-2.31	
	25º-30ºW	0.73	0.39	1.53	1.28	0.16	-0.57	-1.88	-1.62	-0.66	-0.48	-0.05	0.51	-0.66	
	30º-35ºW	0.45	0.27	1.37	0.93	0.06	-0.47	-1.67	-0.84	-0.56	-0.39	-0.05	0.64	-0.26	-8.43
36º-38ºN	10º-35ºW	16.48	12.22	26.09	25.94	9.18	-5.63	-28.31	-38.22	-14.94	-11.63	0.90	11.63		3.77

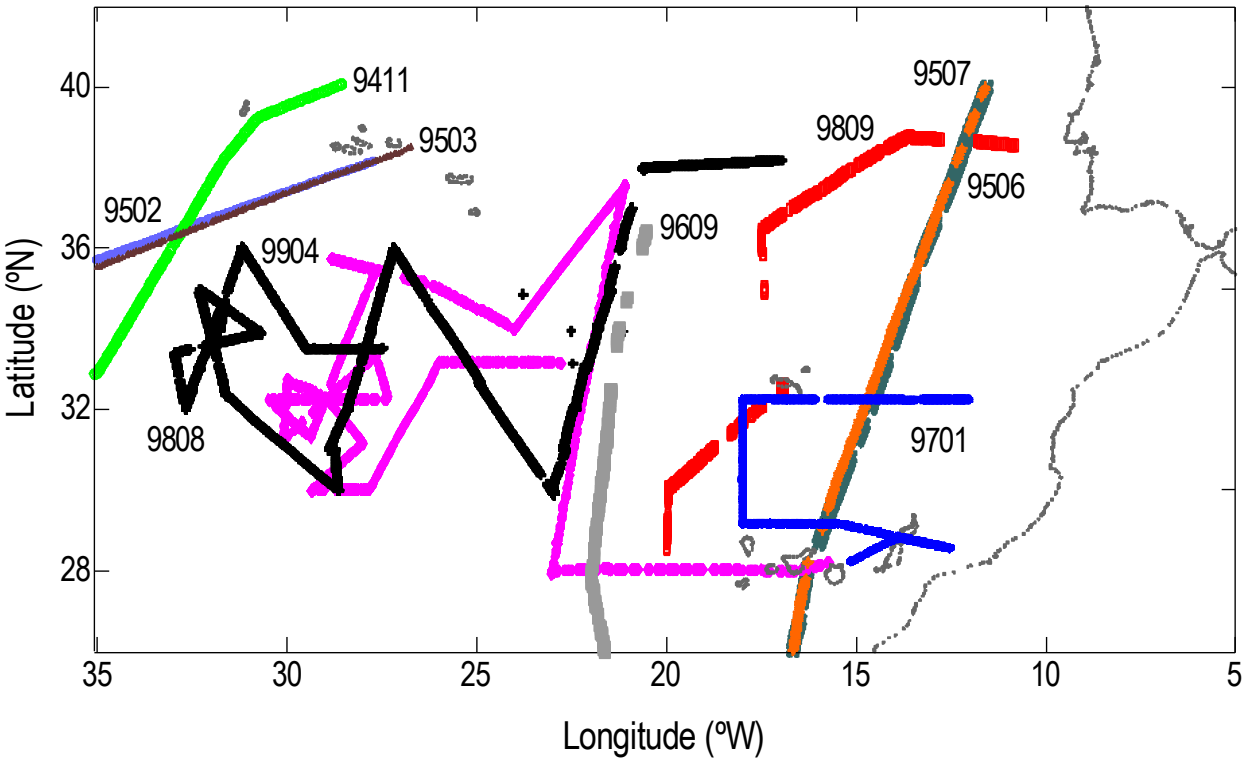

Fig. 1.- Ríos et al. "Seasonal Sea-Surface CO_2 "

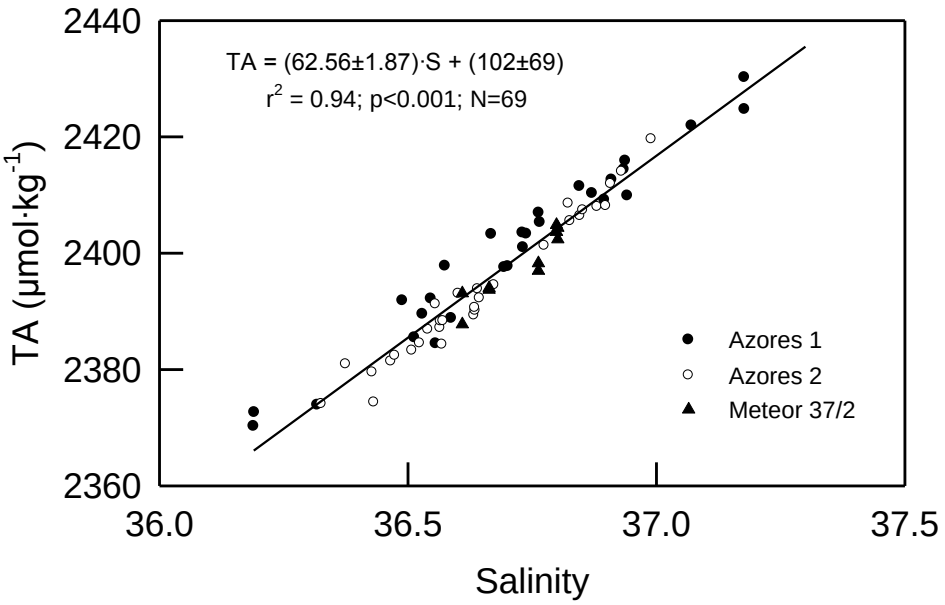

Fig. 2.- Ríos et al. "Seasonal Sea-Surface CO_2 "

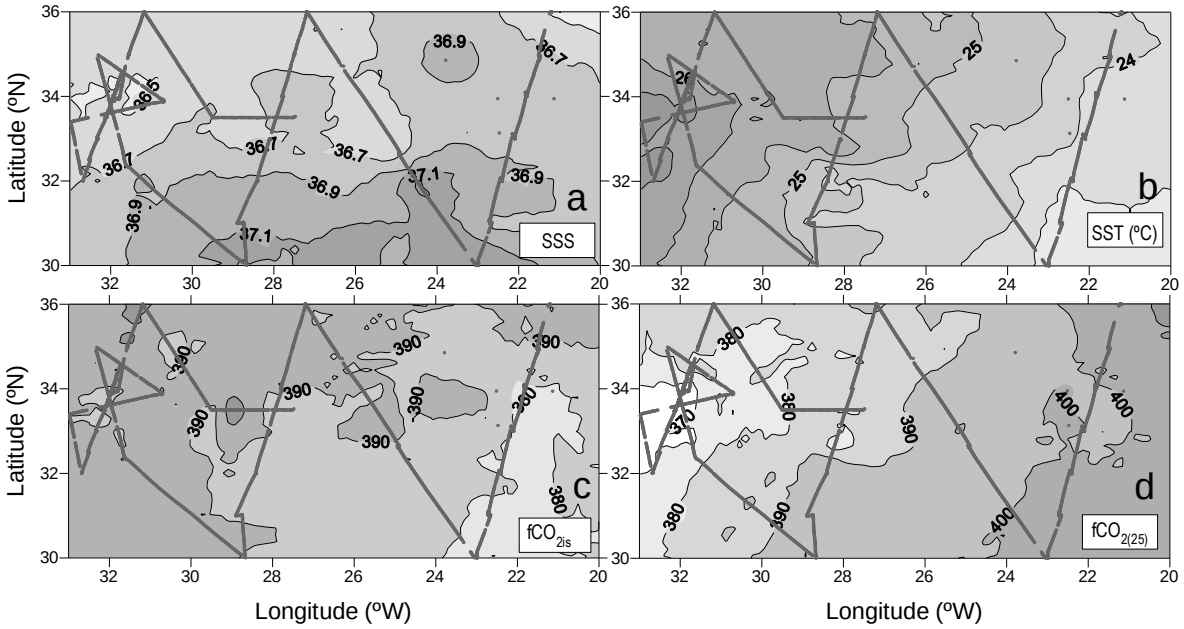

Fig. 3.- Ríos et al. "Seasonal Sea-Surface CO_2 "

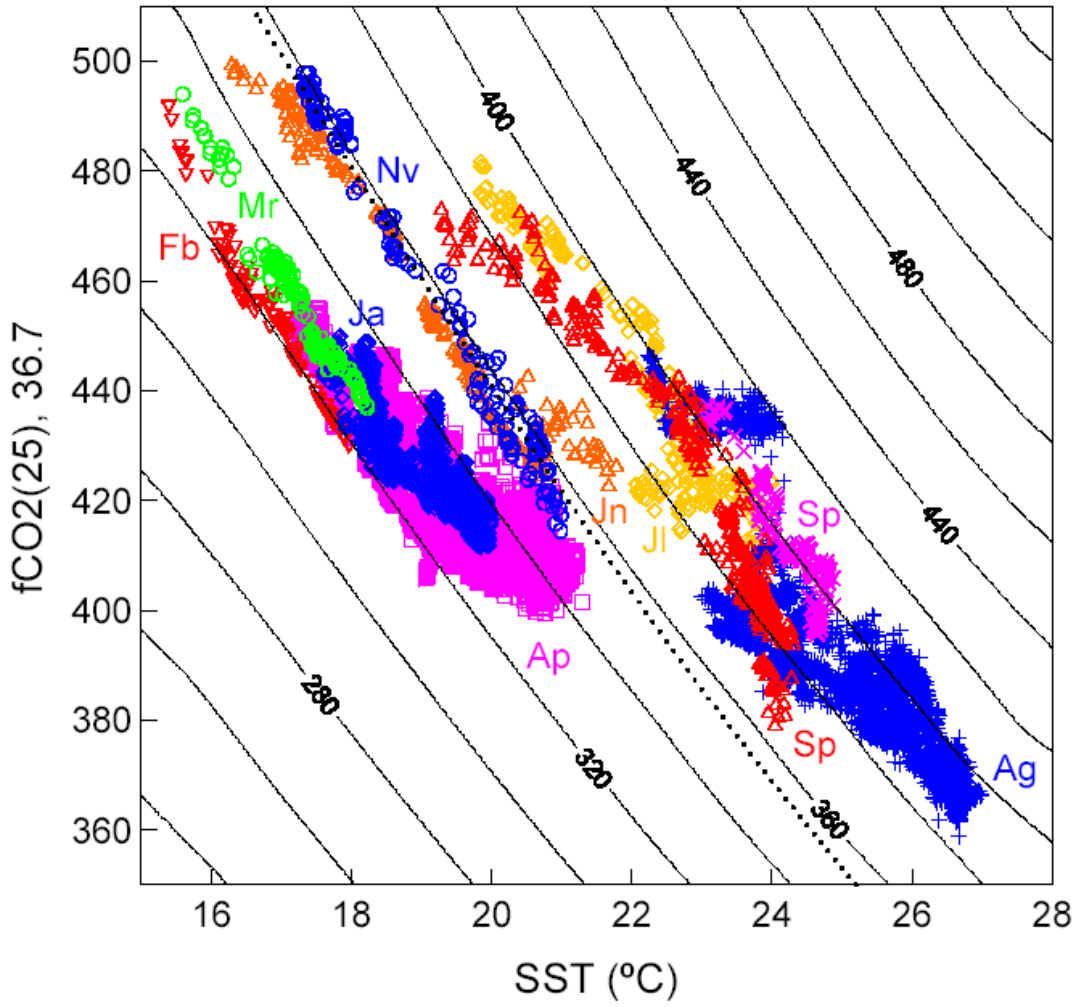

Fig. 4.- Ríos et al. "Seasonal Sea-Surface CO_2 "

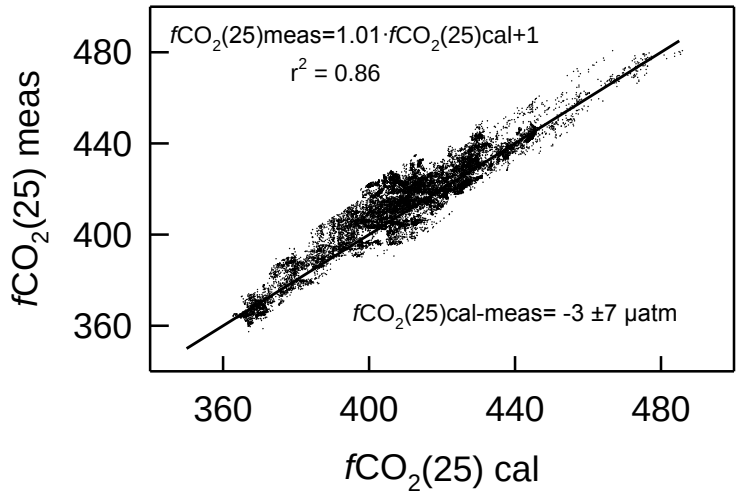

Fig. 5.- Ríos et al. "Seasonal Sea-Surface CO_2 "

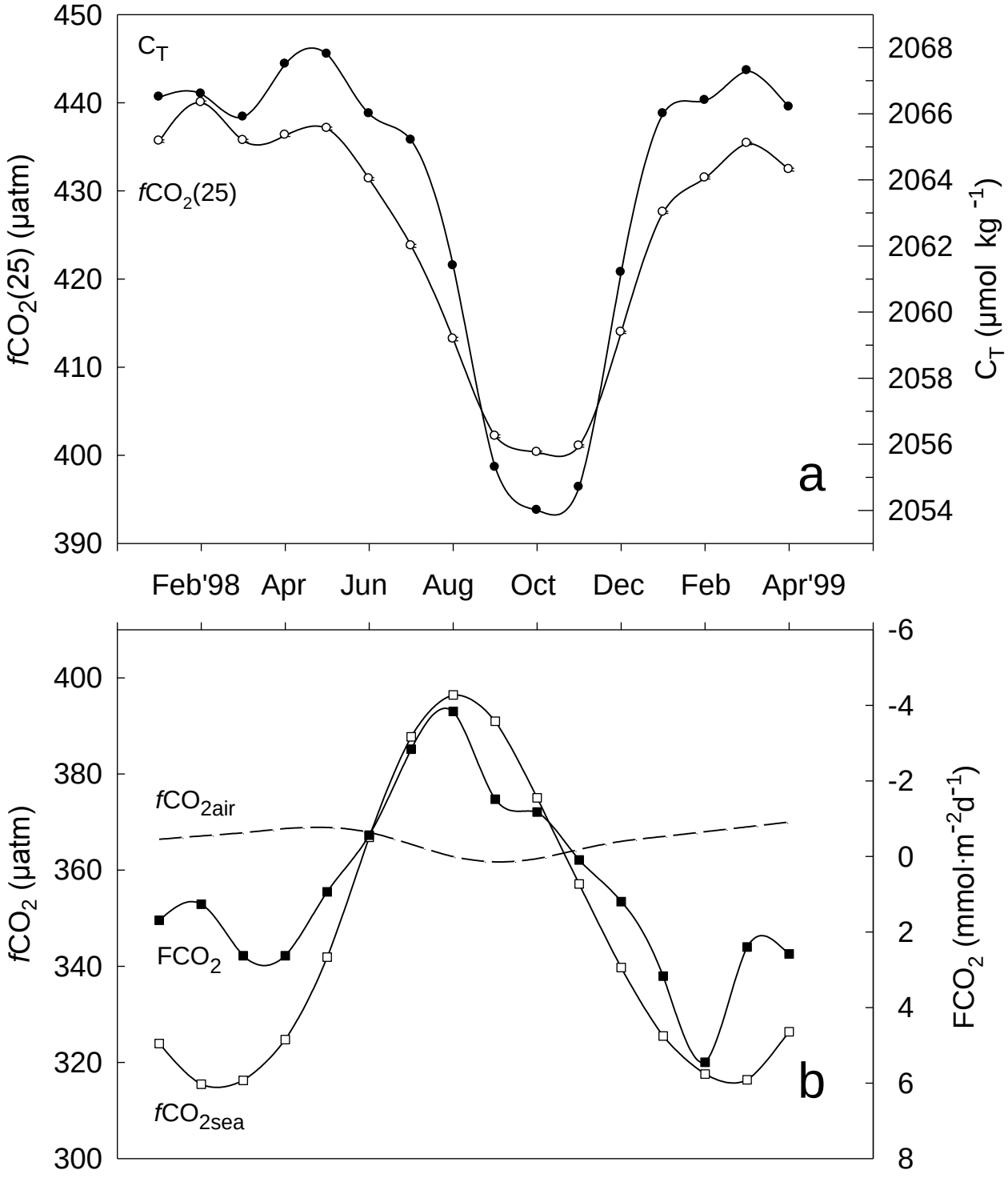
450
440
430
420
410
400
390
C_T
$fCO_2(25)$
$fCO_2(25)$ (µatm)
2068
2066
2064
2062
2060
2058
2056
2054
C_T (µmol kg $^{-1}$)
a
Feb'98
Apr
Jun
Aug
Oct
Dec
Feb
Apr'99
400
380
360
340
320
300
fCO_{2air}
FCO_2
fCO_{2sea}
fCO_2 (µatm)
-6
-4
-2
0
2
4
6
8
FCO_2 (mmol·m^{-2}d^{-1})
b

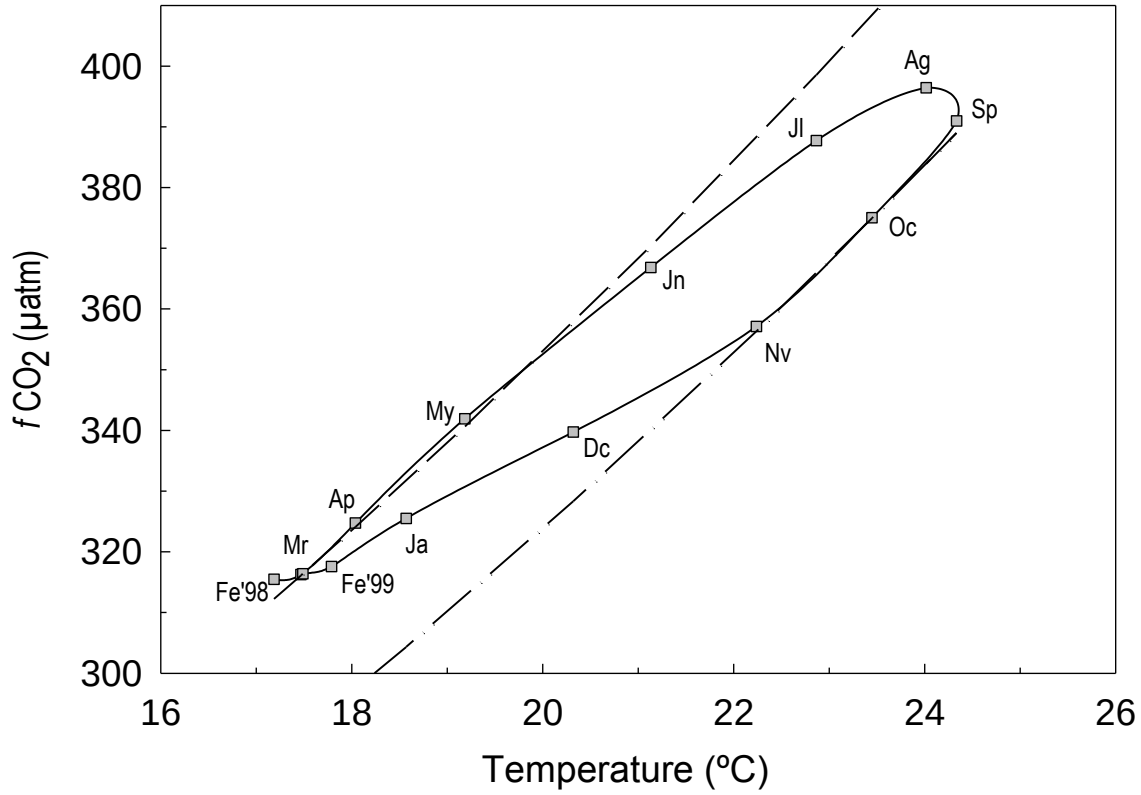

Fig. 7.- Ríos et al. "Seasonal Sea-surface CO_2 "

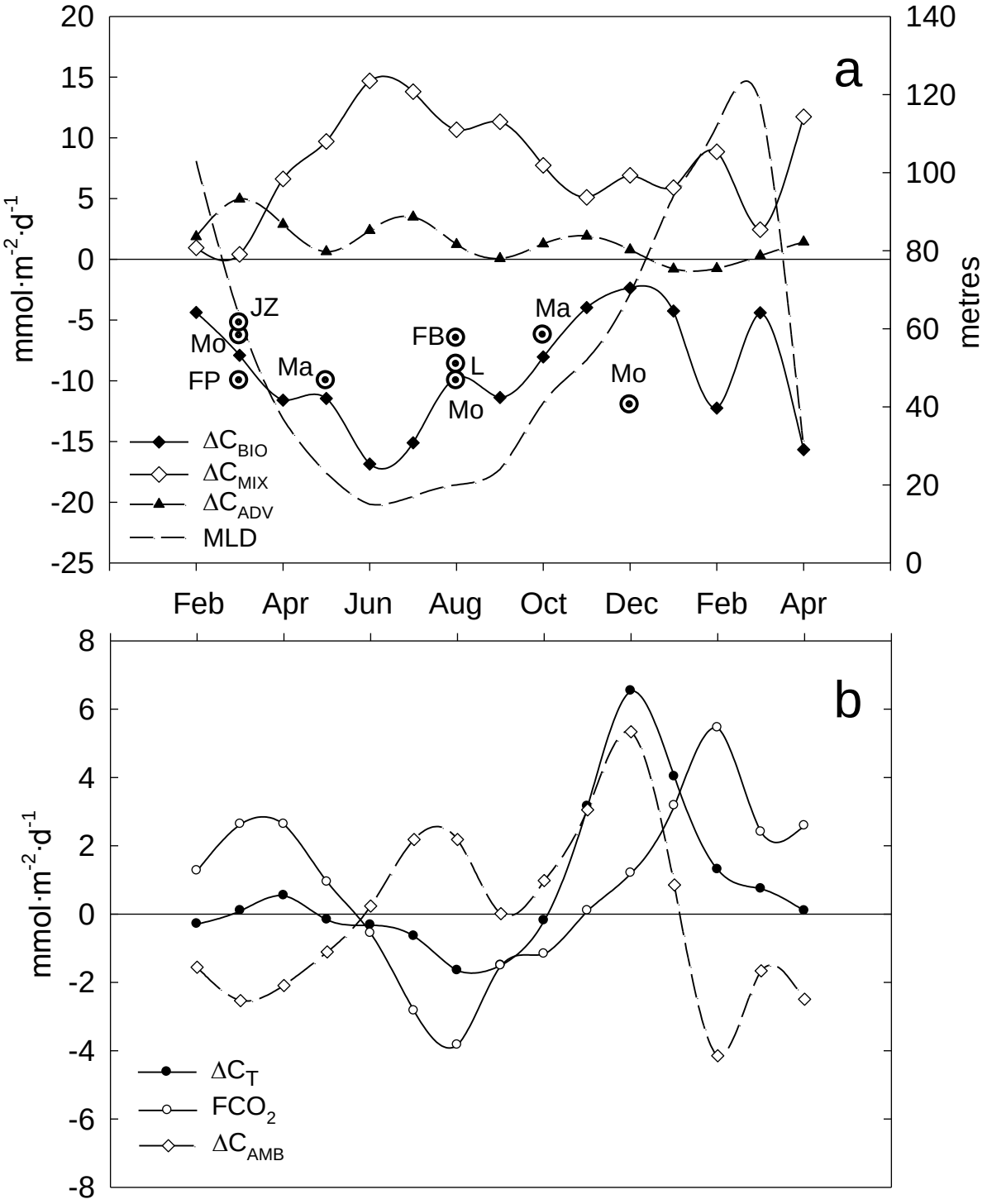

Fig. 8.- Ríos et al . "Seasonal Sea-Surface CO_2 "